

## Large elastic recovery of zinc dicyanoaurate

C. S. Coates, M. R. Ryder, J. A. Hill, J.-C. Tan, and A. L. Goodwin

Citation: [APL Materials](#) **5**, 066107 (2017);

View online: <https://doi.org/10.1063/1.4990549>

View Table of Contents: <http://aip.scitation.org/toc/apm/5/6>

Published by the [American Institute of Physics](#)

---

### Articles you may be interested in

[Thermal conductivity of  \$\text{Bi}\_2\(\text{Se}\_x\text{Te}\_{1-x}\)\_3\$  alloy films grown by molecular beam epitaxy](#)

[APL Materials](#) **5**, 066101 (2017); 10.1063/1.4984974

[Symmetry driven control of optical properties in  \$\text{WO}\_3\$  films](#)

[APL Materials](#) **5**, 066106 (2017); 10.1063/1.4989395

[Vertically aligned diamond-graphite hybrid nanorod arrays with superior field electron emission properties](#)

[APL Materials](#) **5**, 066102 (2017); 10.1063/1.4985107

[Disordered ferroelectricity in the  \$\text{PbTiO}\_3/\text{SrTiO}\_3\$  superlattice thin film](#)

[APL Materials](#) **5**, 066104 (2017); 10.1063/1.4986064

[Oxygen partial pressure dependence of surface space charge formation in donor-doped  \$\text{SrTiO}\_3\$](#)

[APL Materials](#) **5**, 056106 (2017); 10.1063/1.4983618

[Mapping grain boundary heterogeneity at the nanoscale in a positive temperature coefficient of resistivity ceramic](#)

[APL Materials](#) **5**, 066105 (2017); 10.1063/1.4989396

---



## 5 Electronic Measurement Pitfalls to Avoid

Get the whitepaper 

## Large elastic recovery of zinc dicyanoaurate

C. S. Coates,<sup>1</sup> M. R. Ryder,<sup>2</sup> J. A. Hill,<sup>1</sup> J.-C. Tan,<sup>2,a</sup> and A. L. Goodwin<sup>1,a</sup>

<sup>1</sup>*Department of Chemistry, University of Oxford, Inorganic Chemistry Laboratory, South Parks Road, Oxford OX1 3QR, United Kingdom*

<sup>2</sup>*Department of Engineering Science, University of Oxford, Parks Road, Oxford OX1 3PJ, United Kingdom*

(Received 29 April 2017; accepted 15 June 2017; published online 27 June 2017)

We report a single-crystal nanoindentation study of the negative compressibility material zinc(II) dicyanoaurate. The material exhibits a particularly strong elastic recovery, which we attribute to the existence of supramolecular helices that function as atomic-scale springs—storing mechanical energy during compressive stress and inhibiting plastic deformation. Our results are consistent with the relationship noted by Cheng and Cheng [Appl. Phys. Lett. **73**, 614 (1998)] between elastic recovery and the ratio of material hardness to Young's modulus. Drawing on comparisons with other framework materials containing helical motifs, we suggest helices as an attractive design element for imparting resistance to plastic deformation in functional materials. © 2017 Author(s). All article content, except where otherwise noted, is licensed under a Creative Commons Attribution (CC BY) license (<http://creativecommons.org/licenses/by/4.0/>). [<http://dx.doi.org/10.1063/1.4990549>]

Framework materials—solids with structures assembled from a combination of nodes and linkers—are well-known to harbour a variety of interesting mechanical properties.<sup>1</sup> This is especially true for systems with long and flexible linkers, since flexibility generally amplifies mechanical response.<sup>2</sup> One topical example is the broad family of metal–organic frameworks (MOFs), members of which are known to exhibit, e.g., anomalously low elastic moduli,<sup>3</sup> extreme mechanical anisotropy,<sup>4</sup> negative Poisson's ratios,<sup>5</sup> and a propensity for negative linear compressibility (NLC).<sup>6</sup> Taken at face value, these properties suggest a range of attractive applications for open frameworks such as MOFs and MOF-like systems, including in stimuli-responsive materials (sensors), actuators, and shock absorbers.<sup>7,8</sup>

Fundamental studies of framework mechanical response often (rightly) focus on elastic behaviour, and yet the relevance of the elastic regime to practical applications relies on the extent to which plastic deformation can be avoided under application of stress. Often the origin of this stress is an external pressure (e.g., hydrostatic or uniaxial), but guest sorption is an alternative mechanism of particular relevance to MOFs.<sup>9</sup> A key measure of resistance to irreversible deformation is the elastic recovery,  $W_e$ , which quantifies the proportion of work resulting in elastic deformation.<sup>10</sup> Put simply, materials with high elastic recoveries will regain their structure and shape after stress cycling: the elastic recovery of rubber, for example, is nearly unity, whereas brittle ceramics have values of  $W_e$  close to zero. Consequently there is clear merit in developing an understanding of the elastic recovery of open frameworks so as to help predict the extent to which their anomalous mechanical responses might be exploited in practice.

Here we study the elastic recovery of zinc(II) dicyanoaurate,  $\text{Zn}[\text{Au}(\text{CN})_2]_2$ , a MOF-like system known for its extreme NLC behaviour.<sup>11</sup> Whereas the uniaxial compressibilities  $K_\ell = -(\partial \ell / \ell \partial p)_T$  of conventional materials are usually in the range of  $\sim 5\text{--}10 \text{ TPa}^{-1}$  (i.e., a linear contraction of 0.5%–1% for each 1 GPa of applied pressure),  $\text{Zn}[\text{Au}(\text{CN})_2]_2$  exhibits a remarkably large and negative compressibility along the hexagonal axis of its quartzlike structure, with  $K_c = -42(5) \text{ TPa}^{-1}$ .<sup>12</sup> In other words, its structure *expands* on compression by roughly 4% for each GPa. This extraordinary elastic property places  $\text{Zn}[\text{Au}(\text{CN})_2]_2$  in a unique position for application in pressure sensors and shock

<sup>a</sup>Electronic addresses: [andrew.goodwin@chem.ox.ac.uk](mailto:andrew.goodwin@chem.ox.ac.uk) and [jin-chong.tan@eng.ox.ac.uk](mailto:jin-chong.tan@eng.ox.ac.uk)

amplifiers.<sup>13</sup> Yet remarkably little is known regarding its mechanical behaviour beyond its (elastic) compressibility and thermal expansivity.<sup>14</sup> As an experimental technique, nanoindentation methods have provided crucial insight into the mechanical properties of flexible MOFs.<sup>15–17</sup> Consequently we sought to determine the experimental nanoindentation moduli, hardness, and elastic recovery of  $\text{Zn}[\text{Au}(\text{CN})_2]_2$ . Our key result is the discovery of a large elastic recovery, which we attribute to the same supramolecular motifs thought to be responsible for NLC itself.

Before presenting our results we summarise briefly the structural chemistry of  $\text{Zn}[\text{Au}(\text{CN})_2]_2$ . Its crystal structure was first reported in Ref. 18, where the relationship to the structure of  $\text{SiO}_2$ -quartz was clearly noted [Fig. 1(a)]. Like that of  $\beta$ -quartz, the crystal symmetry of  $\text{Zn}[\text{Au}(\text{CN})_2]_2$  is hexagonal, and so from a mechanical perspective the important crystal directions are the [100] and [001] axes. The quartzlike nets of  $\text{Zn}[\text{Au}(\text{CN})_2]_2$  are assembled from tetrahedral  $\text{Zn}^{2+}$  centres, connected via almost-linear dicyanoaurate ( $[\text{Au}(\text{CN})_2]^-$ ) linkers. In this structure, the  $\text{Zn} \cdots \text{Zn}$  distance is so large (*ca* 1 nm) that six separate quartzlike nets interpenetrate.<sup>19</sup> While each net is covalently distinct, neighbouring nets interact via aurophilic ( $\text{Au} \cdots \text{Au}$ ) interactions, the existence of which is inferred from the relatively short  $\text{Au} \cdots \text{Au}$  contacts.<sup>20</sup> These interactions connect to form a set of aurophilic helices lying along directions perpendicular to the hexagonal axis. Variable-pressure crystallographic measurements suggest that the extreme compressibility of this system arises because these aurophilic helices function as supramolecular “springs”.<sup>6</sup> Just as a steel spring is more compressible than steel itself, so too are the aurophilic helices in  $\text{Zn}[\text{Au}(\text{CN})_2]_2$  more compressible than the  $\text{Au} \cdots \text{Au}$  interactions from which they are made. We will come to show that this same supramolecular motif may also be responsible for a strong elastic recovery of the material in these directions.

For our study, we prepared single crystals of  $\text{Zn}[\text{Au}(\text{CN})_2]_2$  using the hydrothermal synthesis approach reported in Ref. 11 (see [supplementary material](#) for details). Nanoindentation measurements were carried out at ambient temperature using an MTS NanoIndenter<sup>®</sup>XP, equipped with a continuous stiffness measurement (CSM) module. The instrument was placed within an isolation cabinet that shielded against thermal instability and acoustic interference. A three-sided pyramidal Berkovich indenter with a sharp tip (end radius  $\leq 50$  nm) was used to measure the indentation modulus and hardness.<sup>21</sup> Calibration was performed using a fused silica standard, with elastic modulus ( $E = 72$  GPa) and hardness ( $H = 9$  GPa). Thermal drifts were ensured to be consistently low. Indentation depth was 2000 nm for all measurements and the inter-indent spacing was typically 35–40  $\mu\text{m}$  to avoid interference between neighbouring indentations. We probed two orientations of  $\text{Zn}[\text{Au}(\text{CN})_2]_2$  crystals, cleaved and polished so as to expose (100) and (001) crystal faces. Continuous stiffness measurement allowed us to collect depth-dependent mechanical data. The indentation modulus was determined

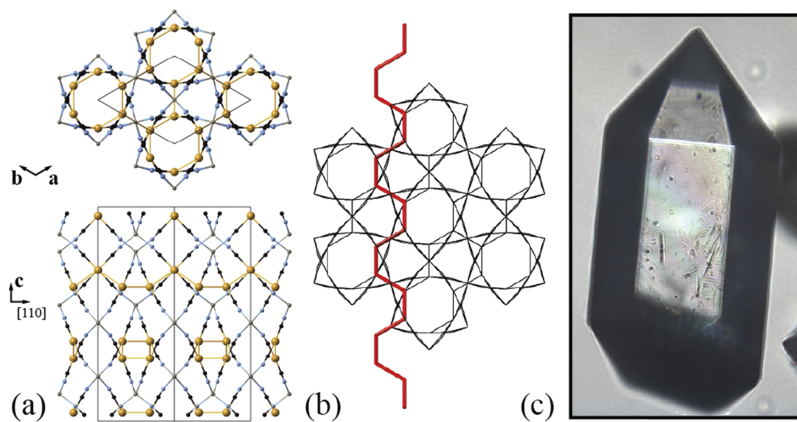


FIG. 1. (a) Representation of the crystal structure of  $\text{Zn}[\text{Au}(\text{CN})_2]_2$ . Zn atoms in gray, C in black, and N in blue, and Au atoms in gold. The top view is parallel to [001]; the bottom view is parallel to [110]. (b) Aurophilic interactions between neighbouring frameworks form helices oriented perpendicular to the hexagonal  $c$ -axis, such as the one shown here in red. (c) The compound crystallises as elongated hexagonal bipyramids. The well-defined crystal facets make  $\text{Zn}[\text{Au}(\text{CN})_2]_2$  an ideal candidate for nanoindentation studies.

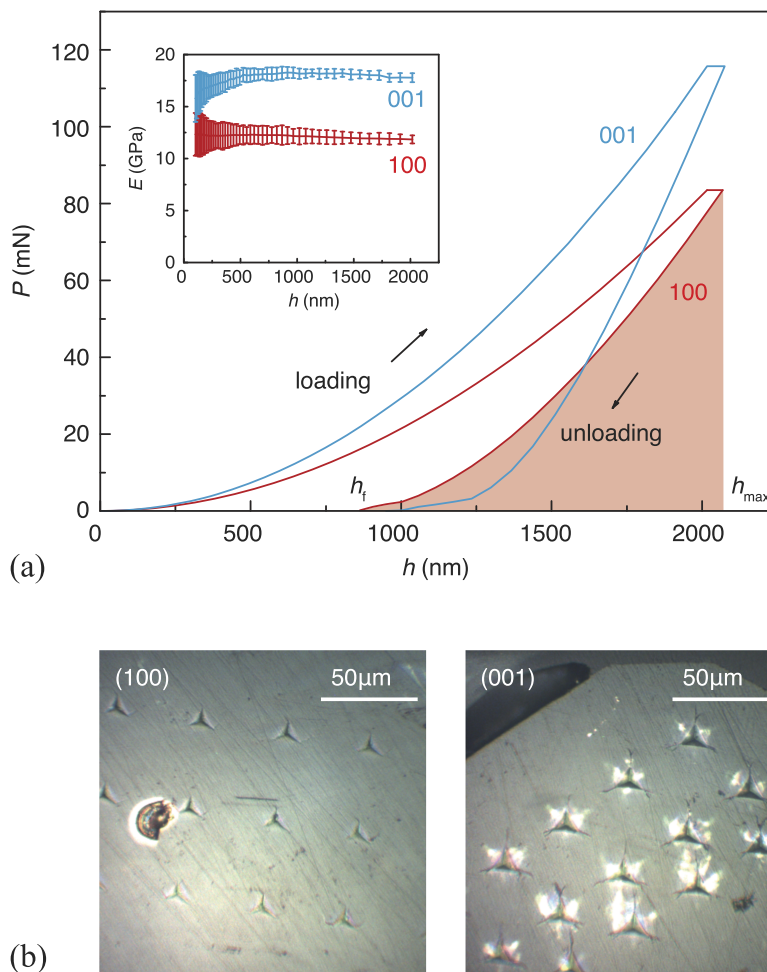


FIG. 2. Typical load–displacement plots obtained from nanoindentation measurements of  $\text{Zn}[\text{Au}(\text{CN})_2]_2$  using the (100) and (001) facets. The elastic recovery  $W_e$  can be calculated from the ratio of the areas under the unloading and loading curves, as described in the text. The inset shows the effective elastic moduli extracted from these data, given as a function of indentation depth  $h$ . (b) Microscopy images of the (100) and (001) surfaces (left and right, respectively) following nanoindentation to a common maximum penetration depth  $h_{\text{max}}$ . Note that the degree of residual deformation is much greater for (001) than for (100); this is consistent with the smaller elastic recovery of the former relative to the latter.

using the Oliver and Pharr method;<sup>22</sup> the hardness was determined by the ratio of the applied pressure and contact area at maximum indentation.

Typical load–displacement curves for  $\text{Zn}[\text{Au}(\text{CN})_2]_2$  are shown in Fig. 2(a). The particular shape of these curves reflects the pyramidal nature of the Berkovich tip used in our study, which results in an increasing contact area at higher loads—and hence decreasing variation in displacement depth on indentation. Our data are characteristic of the nanoindentation response of framework materials, showing contributions from both elastic and plastic deformation;<sup>22</sup> the latter is evident in that loading and unloading curves are not coincident.

Indentation moduli were determined using continuous stiffness measurements on loading, collected for at least twelve crack-free indents for both (100) and (001) crystal faces [inset to Fig. 2(a); see [supplementary material](#)]. Using a representative value of the effective isotropic Poisson's ratio ( $\nu = 0.2$ ), we obtain the values  $E_{100} = 14.5(3)$  GPa and  $E_{001} = 21.4(5)$  GPa; these values vary by not more than 30% when recalculated with alternate values of  $\nu$  (see [supplementary material](#)).

Indentation moduli are not direct measurements of the Young's moduli, but we treat the former as a useful approximation to the latter for the remainder of our analysis (e.g., as in Ref. 22). The moduli are low in comparison with corresponding values for many other coordination polymers<sup>23</sup> but remain higher than the values reported for most porous MOFs.<sup>24</sup>  $\text{Zn}[\text{Au}(\text{CN})_2]_2$  is not porous, and yet its



number density ( $\rho = 0.0512$  atoms  $\text{\AA}^{-3}$ ) shares more in common with open framework materials such as the zeolitic imidazolate framework (ZIF) family of MOFs ( $\rho < 0.08$  atoms  $\text{\AA}^{-3}$ ) than it does with non-porous frameworks ( $\rho > 0.08$  atoms  $\text{\AA}^{-3}$ ). Hence, we suggest that the mechanical behaviour of  $\text{Zn}[\text{Au}(\text{CN})_2]_2$  is MOF-like, despite the absence of any appreciable pore volume in its structure. This borderline behaviour is consistent with the observation that the isostructural material  $\text{Zn}[\text{Ag}(\text{CN})_2]_2$  is known to act as a host for the inclusion of inorganic guests.<sup>25</sup>

The elastic response of  $\text{Zn}[\text{Au}(\text{CN})_2]_2$  shows clear evidence of anisotropy: the elastic modulus along [100] is 32% lower than along [001]. This anisotropy is consistent with the orientation within the crystal structure of aurophilic helices—supramolecular motifs that might be expected to be particularly compliant. *Ab initio* calculations of the Young's moduli arrive at the same conclusion, with  $E_{100}$  lower than  $E_{001}$  by 29% (see [supplementary material](#) for details).

Analysis of load–displacement curves measured during nanoindentation also yields effective hardness values  $H$  in addition to the moduli  $E$ . We find  $H_{100} = 2.23(4)$  GPa and  $H_{001} = 2.19(7)$  GPa, suggesting that hardness is essentially isotropic for  $\text{Zn}[\text{Au}(\text{CN})_2]_2$ . The magnitude of these values is again intermediate to those for dense frameworks, on the one hand, and ZIFs, on the other hand.<sup>26</sup>

Our key finding relates to the elastic recovery,  $W_e$ , which was determined from our nanoindentation measurements by comparing the area under the loading and unloading curves—measures of the work done on indentation or release, respectively<sup>10,27</sup>:

$$W_e = \frac{W_{\text{elastic}}}{W_{\text{total}}} = \frac{\int_{h_f}^{h_{\text{max}}} P_{\downarrow} dh}{\int_0^{h_{\text{max}}} P_{\uparrow} dh}, \quad (1)$$

where  $h_{\text{max}}$  is the maximum tip displacement,  $h_f$  the final tip displacement, and  $P_{\uparrow}(h)$ ,  $P_{\downarrow}(h)$  represent the load applied during loading and unloading cycles at displacement  $h$ .

Figure 2(a) shows clearly that the elastic recovery for indentation in the [100] direction is greater than for the [001] direction. The numerical values we obtain using Eq. (1) are  $W_e = 62.7(3)\%$  and  $43.6(6)\%$  for the (100) and (001) faces, respectively. These values are consistent with the recovery observed directly by inspection of the crystal post-indentation, as shown explicitly in Fig. 2(b). The (100) face shows a much higher resistance to irreversible deformation: the indents are clearly more shallow and show less cracking compared to those for the (001) face. A high elastic recovery leads to improved fracture toughness—i.e., resistance to cracking.<sup>28</sup> Likewise, the degree of material pile-up around residual indents is much greater for the (001) face than for the (100) face, which is consistent with the amplification of material uplift as a result of the formation of cracks.

It is known that there is a linear empirical relationship between  $W_e$  and the ratio  $H/E$  of hardness to Young's modulus.<sup>10,22,29</sup> This relationship allows us to place the elastic recovery behaviour of  $\text{Zn}[\text{Au}(\text{CN})_2]_2$  in the context of that of other MOFs and coordination polymers, by exploiting published  $H$ ,  $E$  data for the ZIF family<sup>30</sup> as well as some dense hybrid frameworks: copper phosphonoacetate (polymorphs 1 and 2, referred to here as CuPA1 and CuPA2),<sup>28</sup> cerium oxalate formate (CeOx),<sup>31</sup> and zinc phosphate phosphonoacetate hydrate (ZnPPA).<sup>32</sup> Our results are shown graphically in Fig. 3, where we have also included in this figure the original data of Ref. 10. What is clear is that the  $W_e$  value we measure for  $\text{Zn}[\text{Au}(\text{CN})_2]_2$  along [100] is amongst the largest for all these systems and is comparable to that of fused silica, which is widely used as a high-recovery standard in nanoindentation studies. The behaviour of  $\text{Zn}[\text{Au}(\text{CN})_2]_2$  along [001] for  $\text{Zn}[\text{Au}(\text{CN})_2]_2$  is typical of a dense hybrid framework, such that the system as a whole behaves like a MOF along **a** but like a dense framework along **c**.

We suggest it is the supramolecular helix motif—instrumental in allowing NLC<sup>6</sup>—that is also responsible for the remarkably high elastic recovery of  $\text{Zn}[\text{Au}(\text{CN})_2]_2$  along [100]. As already discussed, the helix is an object with the particular mechanical property of being able to accommodate bulk compression without substantial compression of the material from which it is constructed. Hence compression of  $\text{Zn}[\text{Au}(\text{CN})_2]_2$  along the [100] direction can in principle be accommodated without substantial changes in any bonding interactions within the solid. In this way, the strain induced during nanoindentation is less likely to result in bond breaking and fracture than

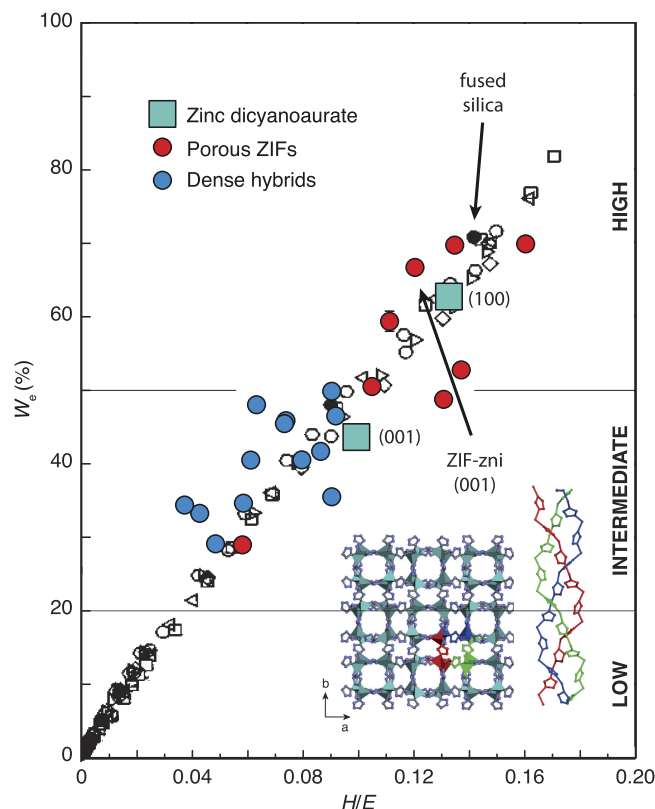


FIG. 3. Empirical relationship between elastic recovery  $W_e$  and  $H/E$ . Data are given for  $\text{Zn}[\text{Au}(\text{CN})_2]_2$  (green symbols), a variety of other porous (red symbols), and dense (blue symbols) framework materials. Also shown are the corresponding data for conventional materials as collated in Ref. 10 (black and white symbols). The data fall naturally into three clusters: systems with low elastic recoveries (brittle ceramics), those with moderate values of  $W_e$  (dense frameworks), and a small set of materials with high, polymer-like elastic recoveries. This last set includes many of the porous ZIFs. Zinc dicyanoaurate behaves as if a dense framework when stress is applied along the hexagonal  $c$  axis but as if an open MOF-type system when compressed along [100]. The insets show a representation of the structures of ZIF-zni as discussed in the text.

might otherwise be the case. Instead the supramolecular springs effectively store the energy transferred during indentation (i.e., work done) and release this energy reversibly upon removal of the indenter tip.

If this is indeed the case for  $\text{Zn}[\text{Au}(\text{CN})_2]_2$ , then it is natural to question whether similar supramolecular motifs may be responsible for strong elastic recoveries in other materials. The data of Ref. 30 reveal that ZIF-zni shows an elastic recovery ( $W_e = 69\%$ ) that is comparable to that found in  $\text{Zn}[\text{Au}(\text{CN})_2]_2$ . At face value, it is perhaps unexpected that this particular member of the ZIF family should show a particularly large value of  $W_e$  since it is both the densest and the least compliant ZIF: its Young's moduli fall in the range  $E = 7.5\text{--}8.5$  GPa.<sup>33,34</sup> The material crystallises in the tetragonal space-group  $I4_1cd$  and within the network are chains of  $\text{Zn}^{2+}$  cations and imidazolate linkers that run along the  $c$ -axis, forming a triple-helical structure as shown in the inset to Fig. 3. By analogy with the arguments presented above, we suggest that this triple helix would also provide a high resistance to permanent deformation. Indeed this triple-helix motif is also found in collagen—crucial supporting components of cartilage, ligaments, tendons, bone, and skin—which itself has a high elastic recovery.<sup>35</sup>

Of course, there are likely to be many other supramolecular motifs—such as hydrogen bonding, or low-dimensional components—that can allow efficient storage of mechanical energy during compression. Nevertheless an interesting future avenue of research would be to explore the elastic recovery properties of helical systems in a broader sense, including elemental solids such as selenium,<sup>36,37</sup> liquid crystals,<sup>38</sup> and supramolecular assemblies.<sup>39</sup> Our key result is that the chemical motif responsible for interesting elastic response (NLC) in  $\text{Zn}[\text{Au}(\text{CN})_2]_2$  also confers resistance

to plastic deformation, establishing helical structures as an attractive motif in the design of resilient materials.

See [supplementary material](#) for a detailed analysis of our nanoindentation data together with a summary of our *ab initio* density functional theory calculations.

C.S.C. and A.L.G. gratefully acknowledge financial support from the E.R.C. (No. 279705) and the Leverhulme Trust (Grant No. RPG-2015-292). J.-C.T. acknowledges research funding from the EPSRC (Nos. EP/K031503/1 and EP/N014960/1). M.R.R. thanks the EPSRC for a DTA postgraduate scholarship, the STFC for a CMSD Award (13-05), and the Rutherford Appleton Laboratory for access to the SCARF cluster.

- <sup>1</sup> B. F. Hoskins and R. Robson, *J. Am. Chem. Soc.* **112**, 1546 (1990).
- <sup>2</sup> W. Li, A. Thirumurugan, P. T. Barton, Z. Lin, S. Henke, H. H.-M. Yeung, M. T. Wharmby, E. G. Bithell, C. J. Howard, and A. K. Cheetham, *J. Am. Chem. Soc.* **136**, 7801 (2014).
- <sup>3</sup> J. C. Tan, B. Civalieri, C.-C. Lin, L. Valenzano, R. Galvelis, P.-F. Chen, T. D. Bennett, C. Mellot-Draznieks, C. M. Zicovich-Wilson, and A. K. Cheetham, *Phys. Rev. Lett.* **108**, 095502 (2012).
- <sup>4</sup> A. U. Ortiz, A. Boutin, A. H. Fuchs, and F.-X. Coudert, *Phys. Rev. Lett.* **109**, 195502 (2012).
- <sup>5</sup> G. N. Greaves, A. L. Greer, R. S. Lakes, and T. Rouxel, *Nat. Mater.* **10**, 823 (2011).
- <sup>6</sup> R. H. Baughman, S. Stafström, C. Cui, and S. O. Dantas, *Science* **279**, 1522 (1998).
- <sup>7</sup> A. E. Aliev, J. Oh, M. E. Kozlov, A. A. Kuznetsov, S. Fang, A. F. Fonseca, R. Ovalle, M. D. Lima, M. H. Haque, Y. N. Gartstein, M. Zhang, A. A. Zakhidov, and R. H. Baughman, *Science* **323**, 1575 (2009).
- <sup>8</sup> G. M. Spinks, G. G. Wallace, L. S. Fifield, L. R. Dalton, A. Mazzoldi, D. De Rossi, I. I. Khayrullin, and R. H. Baughman, *Adv. Mater.* **14**, 1728 (2002).
- <sup>9</sup> S. Krause, V. Bon, I. Senkovska, U. Stoeck, D. Wallacher, D. M. Többsens, S. Zander, R. S. Pillai, G. Maurin, F.-X. Coudert, and S. Kaskel, *Nature* **532**, 348 (2016).
- <sup>10</sup> Y.-T. Cheng and C.-M. Cheng, *Appl. Phys. Lett.* **73**, 614 (1998).
- <sup>11</sup> A. B. Cairns, J. Catafesta, C. Levelut, J. Rouquette, A. van der Lee, L. Peters, A. L. Thompson, V. Dmitriev, J. Haines, and A. L. Goodwin, *Nat. Mater.* **12**, 212 (2013).
- <sup>12</sup> H. L. Zhang, S. Lu, M. P. J. Punkkinen, Q.-M. Hu, B. Johansson, and L. Vitos, *Phys. Rev. B* **82**, 132409 (2010).
- <sup>13</sup> Z. G. Nicolaou and A. E. Motter, *Nat. Mater.* **11**, 608 (2012).
- <sup>14</sup> A. L. Goodwin, B. J. Kennedy, and C. J. Kepert, *J. Am. Chem. Soc.* **131**, 6334 (2009).
- <sup>15</sup> J. P. Best, J. Michler, J. Liu, Z. Wang, M. Tsotsalas, X. Maeder, S. Röse, V. Oberst, J. Liu, S. Walheim, H. Gliemann, P. G. Weidler, E. Redel, and C. Wöll, *Appl. Phys. Lett.* **107**, 101902 (2015).
- <sup>16</sup> X.-L. Qu, D. Gui, Z.-L. Zheng, R. Li, H.-L. Han, X. Li, and P.-Z. Li, *Dalton Trans.* **45**, 6983 (2016).
- <sup>17</sup> C. L. Hobday, R. J. Marshall, C. F. Murphie, J. Sotelo, T. Richards, D. R. Allan, T. Düren, F.-X. Coudert, R. S. Forgan, C. A. Morrison, S. A. Moggach, and T. D. Bennett, *Angew. Chem., Int. Ed.* **55**, 2401 (2016).
- <sup>18</sup> B. F. Hoskins, R. Robson, and N. V. Y. Scarlett, *Angew. Chem., Int. Ed.* **34**, 1203 (1995).
- <sup>19</sup> S. R. Batten, *Curr. Opin. Solid State Mater. Sci.* **5**, 107 (2001).
- <sup>20</sup> M. J. Katz, T. Rammial, H.-Z. Yu, and D. B. Leznoff, *J. Am. Chem. Soc.* **130**, 10662 (2008).
- <sup>21</sup> E. S. Berkovich, *Ind. Diamond Rev.* **11**, 129 (1951).
- <sup>22</sup> W. C. Oliver and G. M. Pharr, *J. Mater. Res.* **19**, 3 (2004).
- <sup>23</sup> Z. Zhang, X. Jiang, G. Feng, Z. Lin, B. Hu, and W. Li, *J. Solid State Chem.* **233**, 289 (2016).
- <sup>24</sup> D. F. Bahr, J. A. Reid, W. M. Mook, C. A. Bauer, R. Stumpf, A. J. Skulan, N. R. Moody, B. A. Simmons, M. M. Shindel, and M. D. Allendorf, *Phys. Rev. B* **76**, 184106 (2007).
- <sup>25</sup> J. A. Hill, A. L. Thompson, and A. L. Goodwin, *J. Am. Chem. Soc.* **138**, 5886 (2016).
- <sup>26</sup> J. C. Tan and A. K. Cheetham, *Chem. Soc. Rev.* **40**, 1059 (2011).
- <sup>27</sup> T. Miura, Y. Benino, R. Sato, and T. Komatsu, *J. Eur. Ceram. Soc.* **23**, 409 (2003).
- <sup>28</sup> J. C. Tan, C. A. Merrill, J. B. Orton, and A. K. Cheetham, *Acta Mater.* **57**, 3481 (2009).
- <sup>29</sup> A. Bolshakov and G. M. Pharr, *J. Mater. Res.* **13**, 1049 (1998).
- <sup>30</sup> J. C. Tan, T. D. Bennett, and A. K. Cheetham, *Proc. Natl. Acad. Sci. U. S. A.* **107**, 9938 (2010).
- <sup>31</sup> J. C. Tan, J. D. Furman, and A. K. Cheetham, *J. Am. Chem. Soc.* **131**, 14252 (2009).
- <sup>32</sup> M. Kosa, J. C. Tan, C. A. Merrill, M. Krack, A. K. Cheetham, and M. Parrinello, *Chem. Phys. Chem.* **11**, 2332 (2010).
- <sup>33</sup> R. Lehnert and F. Seel, *Z. Anorg. Allg. Chem.* **464**, 187 (1980).
- <sup>34</sup> T. D. Bennett, A. L. Goodwin, M. T. Dove, D. A. Keen, M. G. Tucker, E. R. Barney, A. K. Soper, E. G. Bithell, J. C. Tan, and A. K. Cheetham, *Phys. Rev. Lett.* **104**, 115503 (2010).
- <sup>35</sup> K. E. Aifantis, S. Shrivastava, and G. M. Odegard, *J. Mater. Sci.: Mater. Med.* **22**, 1375 (2011).
- <sup>36</sup> D. R. McCann, L. Cartz, R. E. Schmunk, and Y. D. Harker, *J. Appl. Phys.* **43**, 1432 (1972).
- <sup>37</sup> A. B. Cairns and A. L. Goodwin, *Phys. Chem. Chem. Phys.* **17**, 20449 (2015).
- <sup>38</sup> Z.-G. Zheng, Y. Li, H. K. Bisoyi, L. Wang, T. J. Bunning, and Q. Li, *Nature* **531**, 352 (2016).
- <sup>39</sup> E. Yashima, N. Ousaka, D. Taura, K. Shimomura, T. Ikai, and K. Maeda, *Chem. Rev.* **116**, 13752 (2016).